The role of the stagnant-film thickness in mesoscopic modeling of equiaxed grain envelopes

2016 IOP Conf. Ser.: Mater. Sci. Eng. 117 012014

(http://iopscience.iop.org/1757-899X/117/1/012014)

IOP Conf. Series: Materials Science and Engineering **117** (2016) 012014 doi:10.1088/1757-899X/117/1/012014

The role of the stagnant-film thickness in mesoscopic modeling of equiaxed grain envelopes

Youssef Souhar[1], Valerio F. De Felice[1], Miha Založnik[1], Hervé Combeau[1], Christoph Beckermann[2]

[1] Institut Jean Lamour, CNRS – Université de Lorraine, F-54011 Nancy CEDEX, France
[2] Department of Mechanical and Industrial Engineering, University of Iowa, Iowa City, Iowa 52242, USA

E-mail: youssef.souhar@univ-lorraine.fr

Abstract. The mesoscopic envelope model overcomes the limitations of phase-field methods. It can be applied at larger scales and can include fluid flow at reasonable computing cost. It consists of the description of a dendritic grain by an envelope that links the active dendrite branches. The grain is modelled as an evolving porous medium and the liquid-solid phase change and solute transport are modelled by volume-averaged equations. The velocities of the dendrite tips are determined by the local solute-concentration field in the proximity of the envelope through an analytical stagnant-film model. In this publication, we present our implementation of the model for a binary alloy and we discuss the influence of the stagnant-film thickness, the principal model parameter, on the predicted 3D equiaxed grains by comparisons with the scaling laws for binary-alloy dendrites obtained in recent experiments by Melendez and Beckermann.

1. Introduction

The growth of dendritic (treelike) crystal grains is governed by an intricate interplay between the transport of heat and solute as well as capillary and surface effects. Furthermore, it is influenced by adjacent grains due to the overlap of thermal and chemical species fields emanating from each growing grain. The patterns and the dynamics of the strongly nonlinear growth of solidification microstructures are successfuly studied with phase-field methods. These have been developed into efficient tools giving quantitative results. However, as in any model, their practicable scale of application is limited. To bridge the gap between purely microscopic and macroscopic approaches, several meso-scale models have been proposed [1–4], based on various approximations. The mesoscopic envelope model [5–7] offers an accurate representation of group interactions in dendritic solidification. It can be applied in three dimensions at the scale of several grains at acceptable computing cost. The details of the dendritic structure are not resolved. Instead, the complex morphology is approximated by its envelope and by a field of phase fractions in the interior of the envelope. Also, the selection of the dendrite-tip operating state is not predicted by the model. The growth of the envelope is deduced from the velocities of the dendrite tips, calculated by an analytical LGK-type tip model that is matched to the concentration fields in the stagnant film around the envelope. In the model, the tip selection parameter σ^* is an input parameter coming either from measurements or from phase-field simulations.

The mesoscopic model was previously applied to equiaxed dendritic growth in pure materials [5, 6] and in alloys [7]. It was demonstrated that it can accurately predict envelope

shapes and the growth dynamics of pure-material equiaxed dendrites. In this paper, we aim at validating the model for equiaxed growth of alloys by comparing 3D simulations to the scaling laws for binary-alloy dendrites obtained experimentally by Melendez and Beckermann [8]. We discuss the influence of the main parameter of the model, the stagnant-film thickness, on the accuracy of the prediction of the primary-tip velocity, of the envelope shape and of the internal solid fraction of the grains. We give a recommendation for the stagnant-film thickness that leads to a good approximation of the scaling laws.

2. The mesoscopic envelope-field model

The core idea of the mesoscopic envelope model [5–7] is the description of a dendritic grain by its envelope – a virtual smooth surface that links the tips of the actively growing dendrite branches (see figure 1). The velocity of the envelope growth can thus be calculated from the velocities of the dendrite tips. The growth of the dendrite tips is controlled by the solute flux that they eject into their surroundings and is therefore determined by the local conditions in the proximity of the envelope. The branched dendritic structure inside the envelope is only implied and its details are not resolved; the interior of the envelope is rather described in a volume-averaged sense by a phase-fraction field and other volume-averaged quantities. The phase change that determines the evolution of the structure inside the growing envelope is controlled by the solute exchange with the surroundings of the grain.

The model used to describe the kinetics of the dendrite tips is based on the analytical solution of the growth of a single isothermal parabolic tip in an infinite undercooled melt. The classical Ivantsov solution of this problem, recast by Cantor and Vogel [9] gives the supersaturation Ω_δ of the melt at a finite distance δ from the tip with a curvature radius R_{tip} as a function of the tip Péclet number, $\mathrm{Pe}_C = R_{\mathrm{tip}} V_{\mathrm{tip}}/(2D_{\mathrm{l}})$. In three dimensions the Cantor-Vogel function is

$$\Omega_\delta = \mathrm{Pe}_C \exp\left(\mathrm{Pe}_C\right) \left[\mathrm{E}_1\left(\mathrm{Pe}_C\right) - \mathrm{E}_1\left(\mathrm{Pe}_C\left[1+\tfrac{2\delta}{R_{\mathrm{tip}}}\right]\right)\right]. \tag{1}$$

To determine unique values for the tip velocity and radius, a tip selection criterion is required. In the case of a solutally controlled tip (limit of high Lewis numbers) the selection criterion is

$$R_{\mathrm{tip}}^2 V_{\mathrm{tip}} = \frac{d_0 D_{\mathrm{l}}}{\sigma^*}, \tag{2}$$

where $d_0 = \Gamma/(m_{\mathrm{L}} C_{\mathrm{l}}^* (k_{\mathrm{p}} - 1))$ is the solutal capillary length, σ^* is the selection parameter, Γ is the Gibbs-Thomson coefficient, m_{L} is the liquidus slope, k_{p} is the binary equilibrium partition coefficient, and C_{l}^* is the concentration in the liquid at the tip interface (i.e. the equilibrium liquid concentration at the given temperature). Equations (1) and (2) together give the local tip velocity at any point on the grain envelope. The stagnant-film thickness δ is a model parameter that is discussed in the next section. In the mesoscopic model, the tip growth directions are prescribed since the key physics for selection of the preferential growth directions is not included. Knowing the local branch-tip velocity and direction, the envelope velocity is calculated: $\vec{v}_n = V_{\mathrm{tip}} \vec{n} \cos\theta$, where θ is the angle between the normal to the envelope and the closest of the tip growth directions (i.e. the one forming the smallest angle with the normal).

To track the front that represents the envelope we use the sharp interface tracking method by Sun and Beckermann [10]. In this method the tracked front is given by the iso-surface of the smooth indicator field ϕ at $\phi = \phi_{\mathrm{env}}$. The transition of the field ϕ follows a hyperbolic tangent profile, $\phi(n) = \frac{1}{2}\left[1 - \tanh\left(\frac{n}{2W}\right)\right]$, in the vicinity of the front. The phase-field equation that is used to propagate the field contains a stabilization term (right hand side of Eq. (3)), which ensures that the transition of the field ϕ retains its shape and width W.

$$\frac{\partial \phi}{\partial t} + |\vec{v}_n|\, \vec{n} \cdot \nabla \phi = -b \left[\nabla^2 \phi - \frac{\phi\,(1-\phi)\,(1-2\phi)}{W^2} - |\nabla\phi|\, \nabla \cdot \left(-\frac{\nabla \phi}{|\nabla \phi|}\right)\right], \tag{3}$$

The transport at the mesoscopic scale is described by volume-averaged equations, valid in the whole domain. They are equivalent to the classical volume-averaged macroscopic models [11]. The phase change is described at a microscopic scale, where Scheil assumptions are applied. The diffusion of solute in the solid phase is neglected at the mesoscopic scale. This leads to the following conservation equations for solute mass in the liquid and the solid phase:

$$g_\mathrm{l}\frac{\partial C_\mathrm{l}}{\partial t} = D_\mathrm{l}\nabla\cdot(g_\mathrm{l}\nabla C_\mathrm{l}) + C_\mathrm{l}(k_\mathrm{p}-1)\frac{\partial g_\mathrm{l}}{\partial t}\,; \qquad \frac{\partial(g_\mathrm{s}C_\mathrm{s})}{\partial t} = -k_\mathrm{p}C_\mathrm{l}\frac{\partial g_\mathrm{l}}{\partial t}\,. \tag{4}$$

g_l and g_s are the liquid and solid phase fraction respectively and D_l is the diffusion coefficient in the liquid. This equation is valid inside and outside the envelope. Inside and on the envelope the liquid is assumed to be in thermodynamic equilibrium, such that $C_\mathrm{l} = (T - T_\mathrm{f})/m_\mathrm{L}$, where T is the imposed temperature of the isothermal system. Equation (4) thus gives the liquid fraction inside the envelope. Outside the envelope $g_\mathrm{l} = 1$ and Eq. (4) is reduced to the diffusion equation.

3. Results and discussion

Steinbach et al. [5, 6] demonstrated the validity of the mesoscopic model for a pure substance. In this paper, we study the validity of the model for the growth of an isolated equiaxed grain into an infinite and uniformly supercooled melt for a binary alloy. This is done through comparisons with the recent experiments of Melendez and Beckermann [8]. They observed the same generalised envelope shape across a wide range of concentrations and undercoolings. The correlations were close to those observed for pure materials in microgravity. We can therefore assume that the same generalised envelope shape also holds for a purely solutal dendrite with negligible thermal undercooling. Our comparisons are based on this premise and our validation is done for an isothermal, purely solutally driven growth. The computations were performed for a similar range of solutal undercoolings as the experiments. The supersaturation range found in the experiments was $\Omega_0 = 0.05$–0.45. We performed simulations for $\Omega_0 = 0.05$–0.25. Moreover, this validation is done for purely diffusive conditions, although the experiments of Melendez and Beckermann [8] showed that the influence of natural convection on the primary tip velocity was not negligible. However, the small difference between the scaling laws obtained in these experiments and the scaling laws from micro-gravity experiments for pure materials indicates

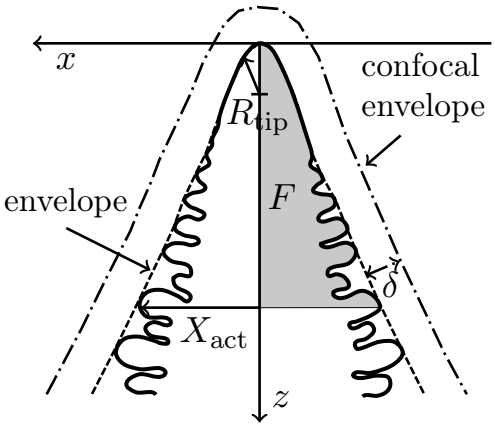

Figure 1. Schematic illustration of the envelope, the confocal envelope, the envelope width X_act and the solid projection area F of an equiaxed dendrite.

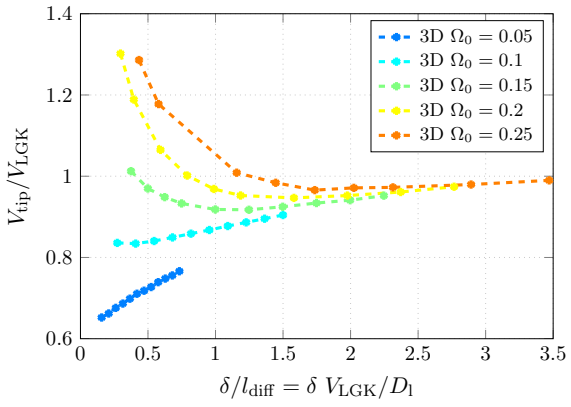

Figure 2. Dependence of the predicted normalised primary-tip velocity on the normalised stagnant-film thickness.

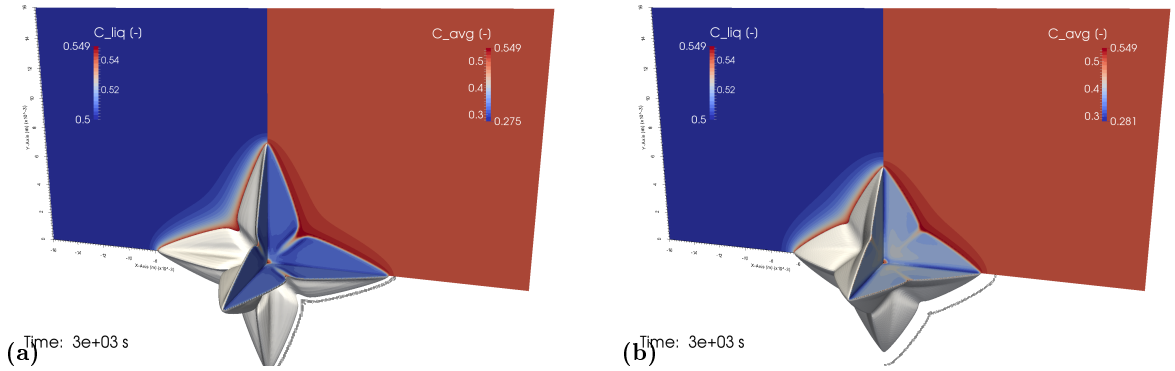

Figure 3. Comparisons of equiaxed grains growing at a supersaturation of $\Omega_0 = 0.1$ for different values of the stagnant-film thickness: (a) $\delta/R_{\mathrm{LGK}} = 5$ and (b) $\delta/R_{\mathrm{LGK}} = 20$.

that the natural convection did not significantly affect the envelope shape in the experiments of Melendez and Beckermann.

We are interested in the tip velocity, the envelope shape, and the solid fraction in the steady state of the dendrite envelope. We can consider that the steady state is reached when both the primary-tip velocity and the envelope shape no longer vary. The theoretical tip velocity and radius, V_{LGK} and R_{LGK}, are calculated with the LGK model, using the same tip selection parameter $\sigma^* = 0.02$ as in the mesoscopic simulations. For purely solutal growth this corresponds to using Eqs. (1–2) with an infinite stagnant-film thickness δ.

The dependence of the primary tip velocity on the stagnant-film thickness for different supersaturations is shown in figure 2. We observed that the best way to scale the stagnant-film thickness is by the diffusion length $l_{\mathrm{diff}} = D_{\mathrm{l}}/V_{\mathrm{LGK}}$. We can see that the steady-state primary tip velocity depends on δ/l_{diff} due to the matching between the analytical solution and the numerical solute diffusion field. Within a large range of supersaturations the error is less than 20 % when $\delta/l_{\mathrm{diff}} > 1$ and less than 10 % when $\delta/l_{\mathrm{diff}} > 1.5$.

Similarly, if we consider the predicted shape of the equiaxed grains, we can notice in figure 3 that the dimensionless stagnant-film thickness δ/l_{diff} significantly affects the shape of the grain envelope. This influence can be studied by comparing our results with the scaling law determined by Melendez and Beckermann [8], which links the dimensionless sidebranch envelope widths $X_{\mathrm{act}}/R_{\mathrm{tip}}$ with the dimensionless longitudinal distance from the tip z/R_{tip} :

$$\frac{X_{\mathrm{act}}}{R_{\mathrm{tip}}} = 0.84 \left(\frac{z}{R_{\mathrm{tip}}} \right)^{0.85} \tag{5}$$

Except near the tip, where the mesoscopic envelope has no physical meaning, the computed envelopes are in relatively good agreement with the experiments. As can be seen in figure 4, the agreement is better when $\delta/l_{\mathrm{diff}} \leq 1$. However, with a too small stagnant-film thickness, the computed primary-tip velocity becomes less accurate and thus a compromise has to be made.

Melendez and Beckermann [8] determined another interesting scaling law for the projected area F of the solid dendrite structure:

$$\frac{F}{R_{\mathrm{tip}}^2} = 0.58 \left(\frac{z}{R_{\mathrm{tip}}} \right)^{1.77} \tag{6}$$

In our case, this projected area is obtained by first extracting the plane of the ridge of the sidebranches, (i.e. the plane at $y = 0$) and then calculating the area integral of the solid fraction

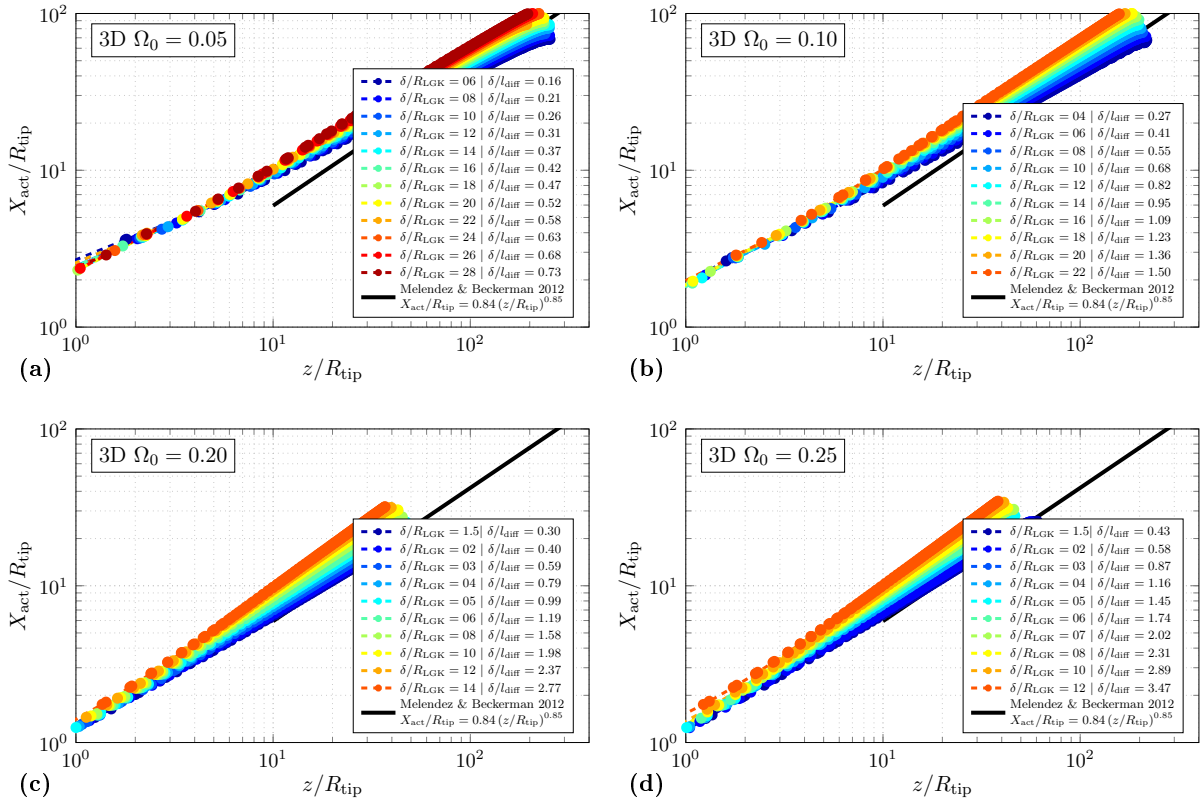

Figure 4. Dimensionless sidebranch envelope width X_{act}/R_{tip} as a function of the dimensionless longitudinal distance from the tip z/R_{tip} and its sensitivity to the stagnant-film thickness δ for four different supersaturations: (a) $\Omega_0 = 0.05$, (b) $\Omega_0 = 0.10$, (c) $\Omega_0 = 0.20$ and (d) $\Omega_0 = 0.25$.

as a function of the distance from the primary tip in this plane. With the notations of figure 1, the projected area is calculated using the formula:

$$F(z) = \int_0^z \left(\frac{1}{X_{act}(z)} \int_0^{X_{act}(z)} g_s(x,z)\,\mathrm{d}x \right) X_{act}(z)\,\mathrm{d}z = \int_0^z \int_0^{X_{act}(z)} g_s(x,z)\,\mathrm{d}x\,\mathrm{d}z \qquad (7)$$

In figure 5, we can see that the internal solid fraction is in very good agreement with the experiments. The exponent factor of the scaling law is very close to the experimentally determined value. For high supersaturations, namely $\Omega_0 = 0.2$ and $\Omega_0 = 0.25$, the pre-factor is also similar. Moreover, we can note that the stagnant-film thickness has little influence on the projected area and finally we can recommend $\delta/l_{diff} = 1$ as a good compromise to obtain realistic simulations with the mesoscopic envelope-field model in terms of envelope shape, internal solid fraction and primary-tip velocity.

4. Conclusions and perspectives

The mesoscopic envelope-field model of solidification gives physically realistic results for equiaxed dendritic growth in binary alloys. We have shown this by comparisons of three-dimensional simulations to experimental results for a wide range of undercoolings. The model can correctly approximate the velocity of both primary and secondary dendrite arms (i.e. the envelope shape) as well as the internal solid fraction in the envelope. To obtain accurate predictions, a proper choice of the stagnant-film thickness, a model parameter, is required. We have shown that a

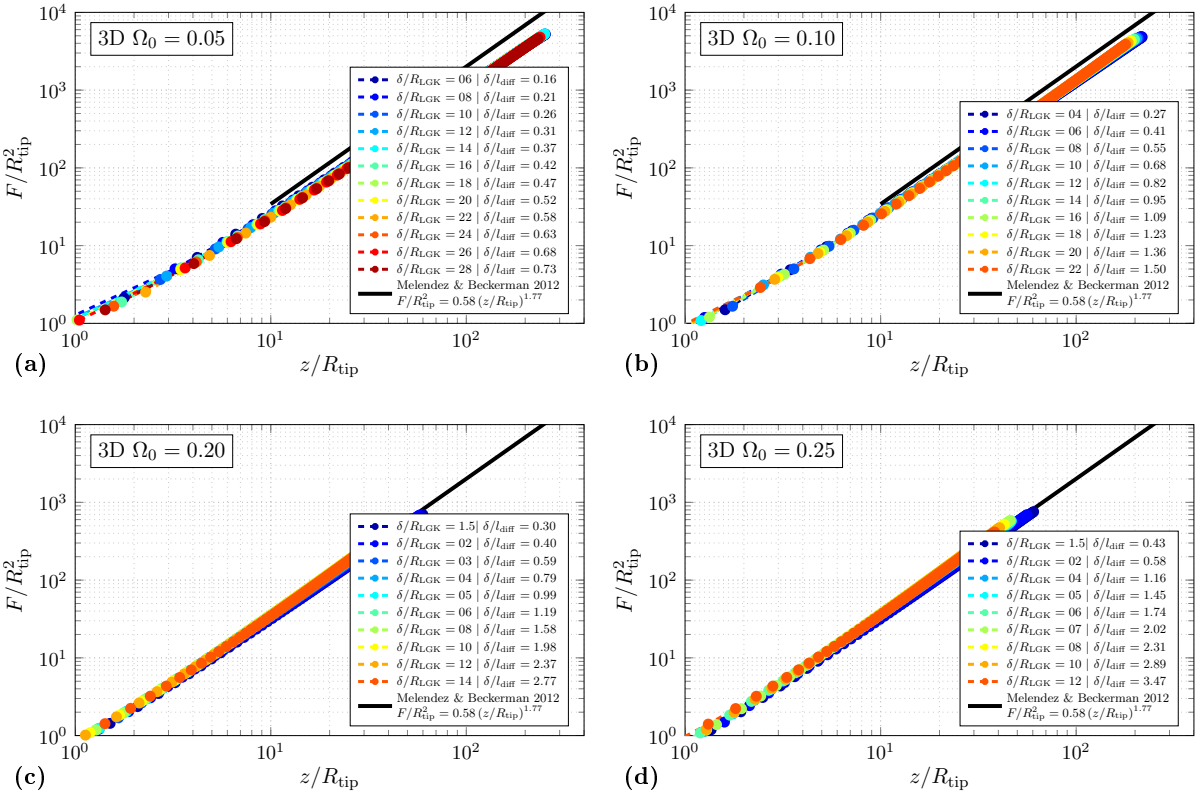

Figure 5. Normalised projection area $F/R_{\rm tip}^2$ as a function of the dimensionless longitudinal distance from the tip $z/R_{\rm tip}$ and its sensitivity to the stagnant-film thickness δ for four different supersaturations: (a) $\Omega_0 = 0.05$, (b) $\Omega_0 = 0.10$, (c) $\Omega_0 = 0.20$ and (d) $\Omega_0 = 0.25$

stagnant-film thickness of the order of the primary-tip diffusion length $D_{\rm l}/V_{\rm tip}$ leads to accurate predictions of the dynamics, of the shape and of the internal solid fraction of equiaxed grains.

Upcoming work will consist of studying interactions between grains with multiple orientations, and of modeling of natural and forced convection, as well as of convection due to grain settling.

Acknowledgement

This work was supported by the French State through the program "Investment in the future" operated by the National Research Agency (ANR), referenced by ANR-11 LABX-0008-01 (LabEx DAMAS) and by NASA under grant number NNX14AD69G.

References

[1] Rappaz M and Gandin C A 1993 *Acta Metall. Mater.* **41** 345–360
[2] Zhu M F and Hong C P 2001 *ISIJ Int.* **41** 436–445
[3] Kharicha A, Stefan-Kharicha M, Wu M and Ludwig A 2012 *IOP Conf. Ser. Mater. Sci. Eng.* **33** 12115
[4] Tourret D and Karma A 2013 *Acta Mater.* **61** 6474–6491
[5] Steinbach I, Beckermann C, Kauerauf B, Li Q and Guo J 1999 *Acta Mater.* **47** 971–982
[6] Steinbach I, Diepers H J and Beckermann C 2005 *J. Cryst. Growth* **275** 624–638
[7] Delaleau P, Beckermann C, Mathiesen R H and Arnberg L 2010 *ISIJ Int.* **50** 1886–1894
[8] Melendez A J and Beckermann C 2012 *J. Cryst. Growth* **340** 175–189
[9] Cantor B and Vogel A 1977 *J. Cryst. Growth* **41** 109–123
[10] Sun Y and Beckermann C 2007 *J. Comput. Phys.* **220** 626–653
[11] Beckermann C and Viskanta R 1993 *Appl. Mech. Rev.* **46** 1–27